4 Improved Bacterial Growth Kinetic Model using Indigenously Isolated Strain *Bacillus Subtilis* MN372379 in the Degradation of Congo Red Dye

The scale-up and optimization of biological processes require detailed knowledge of the bacterial growth kinetics to achieve an economical treatment of the dyeing wastewater. Generally, bacterial growth includes four significant phases known as the *lag* phase, *log* phase, *stationary* phase, and *death* phase. The lag phase indicates the period from inoculation to the 'beginning' of bacterial multiplications. The bacterial growth primarily takes place in the log phase, beyond which the net growth ceases to change (i.e., stationary phase), and finally, it declines in the death phase. The initial part of the log phase is called the *accelerating* log phase, which is characterized by an 'exponential' bacterial growth with a nearly constant specific growth rate. The final part of the log phase is the 'decelerating' log phase, wherein the growth rate starts to decline due to either lack of essential nutrients or the formation of toxic metabolic by-products during substrate utilization or both. Several research works on the modeling of bacterial growth kinetics in the biodegradation of dyeing wastewater have been published in the literature in the last few decades (Talaiekhozani et al. 2015; Sponza and Işık 2004; Monod 1949; Baranyi et al. 1993). However, in most studies, the bacterial growth rates in the log phase were estimated using the exponential growth kinetics applicable only in the accelerating log phase. Few studies barely mentioned the successive decelerating log phase occurring due to inhibition caused by toxic metabolites/ by-products (Waldrop 2009b; Lineweaver and Burk 1934). Understanding and incorporating kinetics of the decelerating log phase is essential to predict a precise overall growth rate of the bacterial mass in the entire log phase. It necessitates an 'accurate' determination of the bacterial growth rate in the log phase to enable maximum degradation of waste materials in a bioreactor.

This study identified an effective bacterial strain (submitted at the National Centre for Biotechnology Information (NCBI), United States as *Bacillus subtilis* MN372379). The *B. subtilis MN372379* was isolated from the pool of bacteria present in the soil samples obtained

from the dyeing waste-discharge site (25.3805° N, 82.5677° E) of a carpet dying unit located at Bhadohi, in Uttar Pradesh, India. The isolated bacteria were used to study the bacterial growth kinetics in the degradation of simulated wastewater containing Congo Red dye in a batch reactor. The main emphasis was on developing a bacterial growth model that incorporated the kinetics of the entire log phase, including the decelerating growth phase. Specifically, a time-averaged specific growth rate for the entire sigmoidal log phase was determined and used in the process optimization to achieve maximum substrate utilization. The average specific growth rate proposed in this study accounted for the decelerated log phase, which was not considered in the conventional exponential growth kinetic applicable only in the accelerating log phase. The nature of metabolite inhibition in the decelerating phase was also examined. Further, the computed time-averaged bacterial growth rate was incorporated in various substrate inhibition models to account for the metabolite- and substrate-, inhibitions. Finally, the effect of process parameters such as the initial dye loading and inoculum size on the dye utilization rate was also investigated.

4.1 The conventional approach to determine the bacterial growth rate

A general rate law for the bacterial growth kinetics in the log phase can be written as

$$\frac{dX}{dt} = k\, f(S)\, g(X) \qquad (4.1)$$

where X (g/L) is the biomass concentration, S (mg/L) is the substrate concentration, t (hr) is time, k is the rate constant and, f and g are general functions of S and X, respectively. Considering the complex nature of the biological processes, it is extremely difficult to derive a general rate expression in the form of Eq 4.1. Jacques Monod (Monod 1949; Baranyi et al. 1993) assumed that the growth rate in the log phase has a first-order dependence on the biomass concentration and proposed the following rate law for bacterial growth.

$$\frac{dX}{dt} = \mu^{bg}(t).X = \mu_{max}^{bg}\left(\frac{S(t)}{K_d+S(t)}\right)X \qquad (4.2)$$

where μ^{bg} (hr^{-1}) is termed as the *specific* bacterial growth rate in the log phase and is defined as $\frac{1}{X}\frac{dX}{dt}$; μ_{max}^{bg} (hr^{-1}) is the maximum specific growth rate, and K_d (mg/L) is the half-saturation constant. It is apparent on the comparison of Eq 4.1 and Eq 4.2 that the $f(S)$ was assumed to be in the form of $\left(\frac{S}{K_d+S}\right)$ in Monod's model. The magnitude of $f(S)$ would increase from zero to one as the substrate becomes abundant from rare. Monod's rate law for bacterial growth follows a zero-order dependence on the substrate concentration when the substrate is abundant. Therefore, Monod expression *does not* account for inhibition in the bacterial growth caused at high substrate concentration. The substrate inhibition was considered in various models present in the literature (Tsai et al. 2013; Monteiro, Boaventura Ra Fau - Rodrigues, and Rodrigues; Kureel et al.; Geed et al.; Arutchelvan et al.), including the popular ones given by Andrew-Haldane (Andrews 1968), Aiba (Aiba S Fau - Shoda, Shoda M Fau - Nagatani, and Nagatani), and Edwards (Edwards 1970) which are discussed elsewhere in this study.

Further, it should be noted that Eq 4.2 cannot be integrated directly to determine biomass concentration as a function of time, *X(t)*, until the substrate concentration, *S(t)*, is known. If the change in *S* is assumed to be negligible (this may be true at the beginning of the accelerating log phase where the substrate is present in sufficient amount), Eq 4.2 can be rewritten as

$$\frac{dX}{dt} = \mu_a^{bg} X = \left[\mu_{max}^{bg}\left(\frac{S_0}{K_d+S_0}\right)\right] X \qquad (4.3)$$

where μ_a^{bg} is the initial specific bacterial growth rate in the accelerating log phase, S_o (mg/L) is the initial substrate (i.e., dye, in the context of this study) concentration. Eq 4.3 can now be integrated to obtain the well-known exponential kinetic expression for bacterial growth as

$$X = X_o e^{\left(\mu_a^{bg} t\right)} \quad \text{or} \quad \ln X = \mu_a^{bg}.t + \ln X_o \qquad (4.4)$$

It is emphasized that a constant value of μ_a^{bg} obtained from Eq 4.4 would hold good only for the initial part of the accelerating log phase (as shown in Figure 4.1), where the change in the substrate concentration is not significant. However, there are many studies published in the literature that determined specific bacterial growth rates (either by Monod's model or various substrate inhibition models) using the initial substrate concentrations without mentioning that the μ^{bg} obtained in their studies was applicable only for the initial part of the "accelerating" log phase (Sen and Sarkar; El-Sheekh, Gharieb, and Abou-El-Souod 2009; Agarry, Audu, and Solomon 2009).

4.2 Time-Averaged Bacterial Growth Rate Incorporating the Metabolite Inhibition: an Improved Approach Proposed in the Present Study

It is clear now that the value of μ_a^{bg} would not be constant throughout the log phase as is considered in the conventional approach (Eq. 4.3 & 4.4). It would decrease as the bacterial growth progresses towards the decelerating log phase. In this study, a *time-weighted* average specific growth rate is determined for the entire log phase, including the decelerating phase to account for the *metabolite-inhibition*. The complete sigmoidal log phase is discretized in uniform time steps of Δt (hr) as shown in parts 2 & 3 of the growth curve in Figure 4.1.

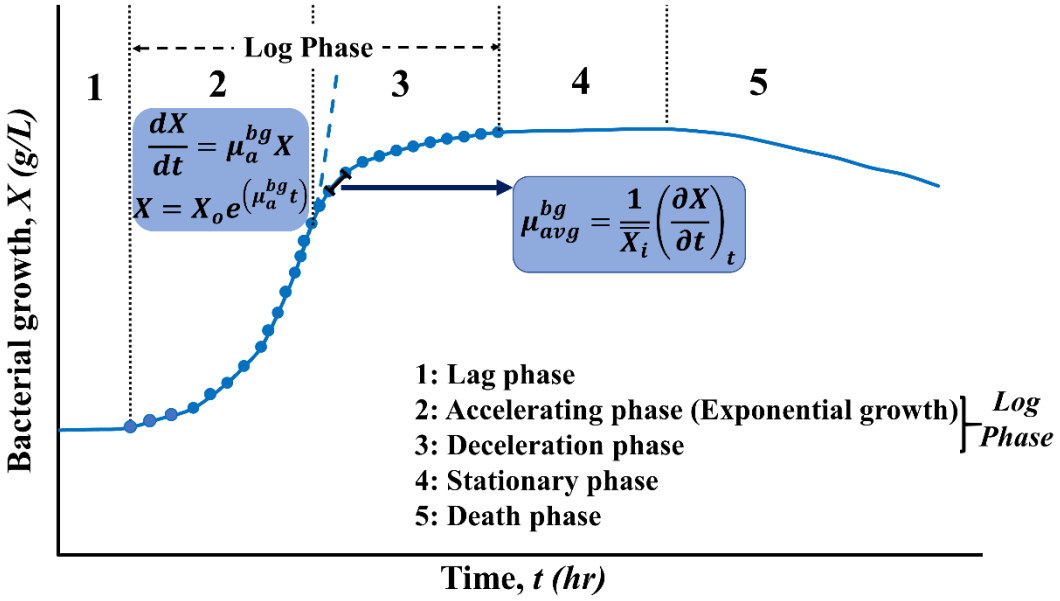

Figure 4.1 Schematic showing the approach used in this study to determine time-averaged specific growth rate for the entire sigmoidal log phase comprised of the accelerating log phase (represented by an exponential growth curve) and the decelerating log phase (represented by growth with inhibition caused by the metabolic toxicants)

The specific growth rate is calculated at each time step and summed up across the entire accelerating and decelerating phases to determine an average specific growth rate for the log phase as follows:

$$\mu_{avg}^{bg} = \frac{1}{t_{log}^{total}}\left(\sum_{\forall i,log}\left[\frac{1}{\overline{X}_i}\left(\frac{\partial X}{\partial t}\right)_i\right]\Delta t\right) = \frac{1}{t_{log}^{total}}\left(\sum_{\forall i,log}\left[\frac{X_{i+1}-X_i}{(X_{i+1}+X_i)/2}\right]\right) \qquad (4.5)$$

where μ_{avg}^{bg} (hr^{-1}) is the average specific bacterial growth rate for the entire log phase; X_i and X_{i+1} are the biomass concentration at i^{th} and $(i+1)^{th}$ time steps, respectively; $\overline{X}_i$ (g/L) is the average biomass concentration at i^{th} time step; and t_{log}^{total} is the total duration of the log phase, including the accelerating and decelerating phases. The μ_{avg}^{bg} determined in this manner would account for the accelerated and decelerated growth fractions in the log phase, as shown in Figure 4.1. Therefore, the μ_{avg}^{bg} should ideally be maximized in a process optimization study aiming to enhance bacterial growth.

4.3 Time-averaged substrate utilization rate: An approach proposed in the present study

The goal of process optimization of a biodegradation reaction in a bioreactor is to maximize substrate utilization at minimum cost. The specific degradation rate of the substrate (also known as the *specific substrate utilization rate*, μ^{su}) is defined as the rate of change of substrate concentration per unit biomass as:

$$\mu^{su} = \frac{1}{X}\left(-\frac{\partial S}{\partial t}\right) \tag{4.6}$$

The μ^{su} is determined from the measured substrate, *S(t)*, and bacterial, *X(t)*, concentration profiles in a biodegradation process as shown in Figure 4.2. It is apparent from the figure that the substrate degradation rate $\left(\frac{\partial S}{\partial t}\right)$ and the bacterial concentration (X) would change with time in the log phase. Therefore, a time-averaged specific substrate utilization rate (μ_{avg}^{su}) over the entire log phase (including the accelerating and decelerating phases) is determined in this study as follows:

$$\mu_{avg}^{su} = \frac{1}{t_{log}^{total}} \int_{log} \frac{1}{X}\left(-\frac{\partial S}{\partial t}\right) dt = \frac{1}{t_{log}^{total}} \left(\sum_{\forall i,log} \frac{(S_i - S_{i+1})}{\left(\frac{X_i + X_{i+1}}{2}\right)} \right) \tag{4.7}$$

In this study, the process parameters (such as the initial substrate concentration and initial inoculum size) were optimized to achieve maximum μ_{avg}^{su}.

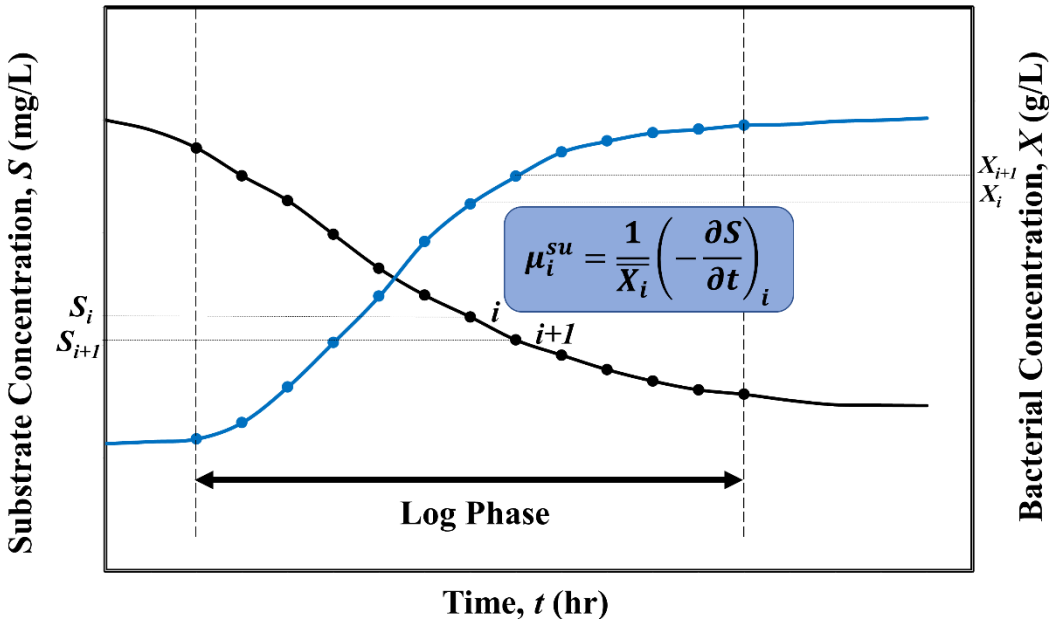

Figure 4.2 Schematic showing the approach to determine a time-averaged specific substrate utilization rate for the log phase using the measured substrate concentration profiles and bacterial mass

4.4 Identification of the Efficient Dye-Degrading Bacterial Isolate

The decolorization potential of all the 10 morphologically distinct isolates was examined with the simulated dye-water of 100 mL containing 50 mg/L of Congo red dye. Four milliliters of inoculum of each isolate were taken in this study, and the decolorization of the dye-water with each isolate was monitored for 72 h. The percentage removal of dyes in all cases was determined, presented in Table 4.1. The isolate "I" was found to offer the maximum dye removal efficiency. The isolate "I" was subjected to 16S rRNA sequencing for molecular characterization and found to be 99.76% matching with *Bacillus subtilis subs. stercoris*, for which a phylogenetic tree has been presented in Figure 4.3. The nucleotide sequence results obtained from the 16S rRNA sequencing method have been submitted to the NCBI GenBank®, a genetic sequence database, under the accession number MN 372379. The isolate "I" was used for further bacterial growth and dye utilization experiments presented in this study.

Table 4.1 Percentage removal of Congo red dye with 10 different bacterial isolates

Bacterial Isolate	A	B	C	D	E	F	G	H	I	J
% Dye Removal	57.84	33.73	39.01	64.31	66.58	57.16	44.51	38.04	70.72	36.68

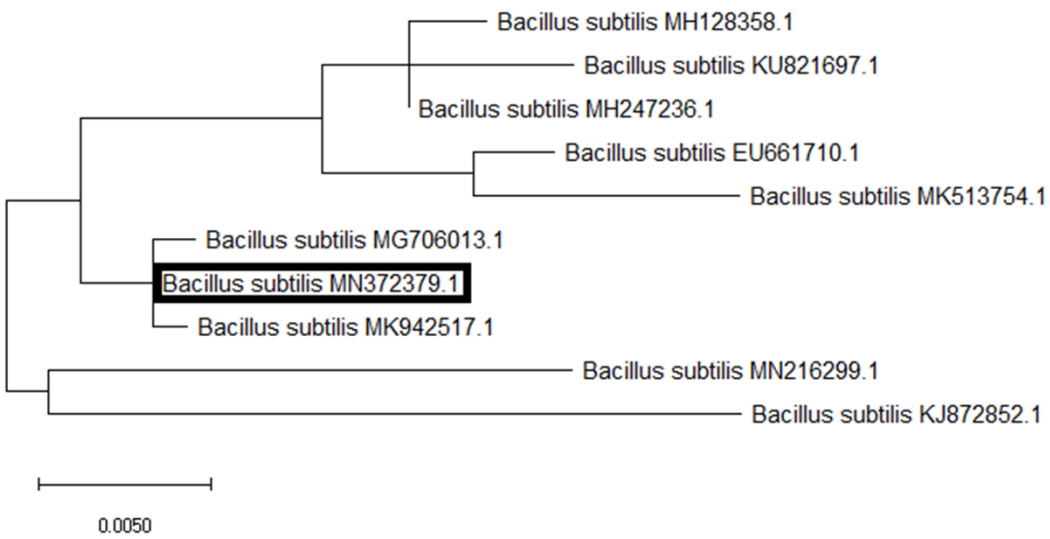

Figure 4.3 Phylogenetic tree obtained from MEGA X 10.1 showing the evolutionary history using the neighbor-joining

4.5 Bacterial Growth Kinetics

4.5.1 Degradation of the Synthetic Wastewater at Different Initial Dye Concentrations

The degradation experiments of Congo Red dye were conducted in a batch reactor for 72 hours with the initial inoculum size of 4% (v/v) of the isolate *I* (with 7.68 x10^8 CFU/mL) at varied initial dye concentrations of 50-250 mg/L. The bacterial dry cell mass (biomass concentration) and dye (i.e., substrate) concentration were measured at different time steps and are presented in Figure 4.4 Biomass concentration (g/L) and dye concentration (mg/L) in the batch reactor at different time steps for various initial dye concentrations of (a) 50 mg/L, (b) 100 mg/L, (c) 150 mg/L, (d) 200 mg/L, and (e) 250 mg/L. It is apparent from the plots that the lag phase ends (and the exponential growth phase starts) after 8 to 16 hours. The lag phase duration was found to be increasing from 8 to 16 hours when the initial dye concentration was increased from 50 to 250 mg/L. The biomass growth reached up to 8 gm/l under 100 mg/l of

dye concentration compared to 10 gm/l under 250 mg/l of dye in the decelerating log phase. Although a higher amount of biomass was formed in the case of 250 mg/l of dye, the growth rate was reduced compared to lower dye concentration. It indicates that the bacterial population took a long to adapt to the toxic environment at high dye concentrations. In the log phase, the decelerating phase, separated from the accelerating exponential phase by a point of inflection in the bacterial growth curve, was observed at all initial dye concentrations in this study. It is apparent from the dye concentration profiles that the substrate (i.e., dye) was always present in the bioreactor even during the decelerated bacterial growth phase. It indicated that the scarcity of substrate was not the cause of inhibition in the growth rate during the deceleration phase. Hence, the cause of deceleration in the bacterial growth rate was attributed to toxic metabolic by-products. A stationary phase is also observed after 40 to 48 hours which denotes the equilibrium between the growth and death rates of the bacteria. As the total bacterial dry cell mass measured in this study included the dead cells, the death phase couldn't get captured in the measurements. The death phase might have been started at some point in the stationary phase.

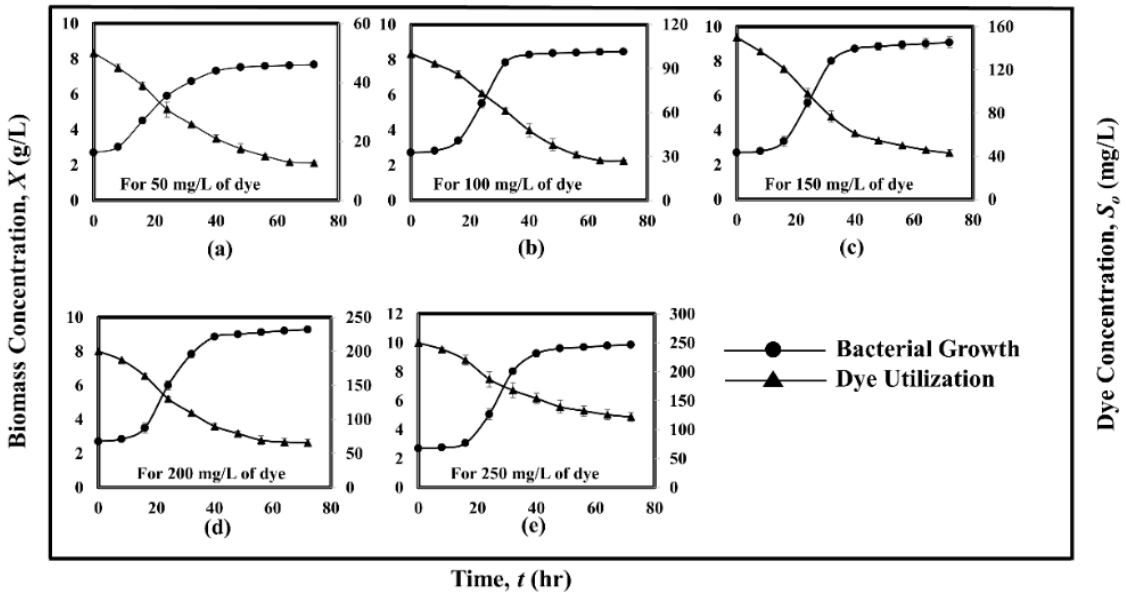

Figure 4.4 Biomass concentration (g/L) and dye concentration (mg/L) in the batch reactor at different time steps for various initial dye concentrations of (a) 50 mg/L, (b) 100 mg/L, (c) 150 mg/L, (d) 200 mg/L, and (e) 250 mg/L

4.5.2 Determination of the specific bacterial growth rate time-averaged over the entire log phase for incorporating metabolite inhibition

The specific bacterial growth rate (μ^{bg}) was calculated for the accelerating phase (using Eq. 4.4) and the entire log phase (using Eq. 4.5), and they are designated as μ_a^{bg} and μ_{avg}^{bg} respectively. The calculated μ^{bg} are displayed against varied initial dye concentrations in Figure 4.3. The μ_a^{bg} was based on the initial exponential growth phase only and has been conventionally used in the literature. Whereas, the $\mu_{avg}^{bg}$was the time-averaged specific bacterial growth rate determined for the entire log phase. It is apparent from Figure 4.3 that the μ_{avg}^{bg} is significantly lower than the μ_a^{bg}. It indicates that the role of the decelerating phase, which represents the enzyme inhibition caused by the metabolic toxicants, cannot be ignored. A significant drop in the μ_{avg}^{bg}, relative to the μ_a^{bg} in Figure 4.3 implies the presence of a large fraction of decelerating growth in the log phase presented in the corresponding Figure 4.4. The μ_a^{bg} (based on the exponential growth kinetic applicable in the accelerating log phase)

overestimated the specific growth rate by 36-62%, as shown in Table 4.2 for different cases of the initial dye concentrations. It suggests that a time-averaged specific growth rate over the complete log phase should be determined and used to model bacterial growth.

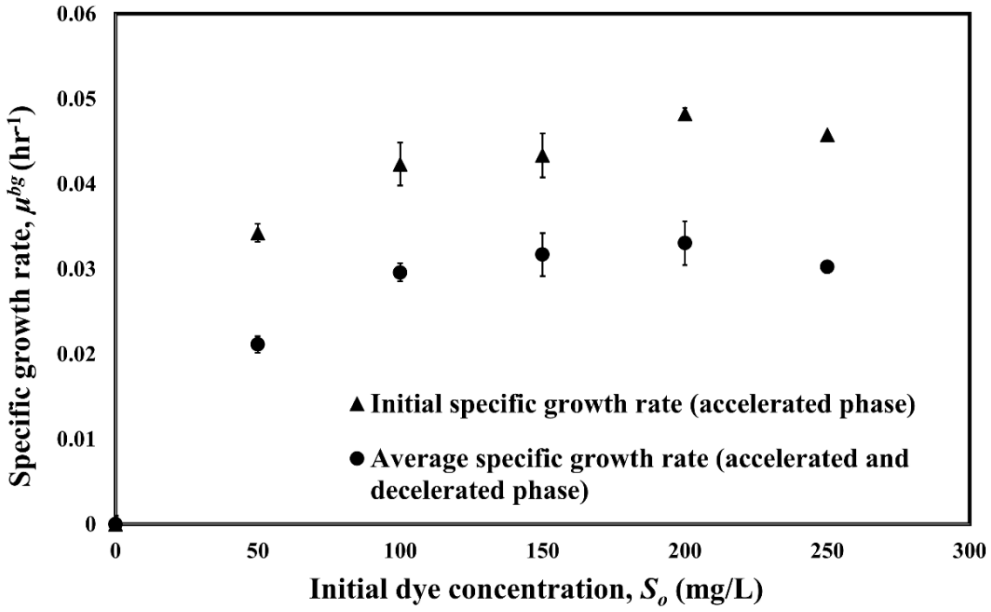

Figure 4.5 Initial specific growth rate, μ_a^{bg}, (based on the accelerated exponential growth phase) and the time-averaged specific growth rate, μ_{avg}^{bg}, (accounting both the accelerated and decelerated log phases) against the initial dye concentrations.

Table 4.2 Overestimated in the log phase-specific growth rate when the conventional exponential growth kinetic was assumed (i.e., the decelerating phase was not considered)

Initial dye concentration (mg/L)	Overestimate in the log phase-specific growth rate (%)
50	61.93 ± 2.79
100	43.07 ± 3.12
150	36.78 ± 2.92
200	45.96 ± 4.03
250	51.41 ± 2.35

4.5.3 Nature of metabolite inhibition in the decelerating part of log phase

The inhibition in the decelerating log phase due to excess metabolic by-products has been discussed in section 4.2. The nature of metabolite inhibition in the decelerating phase is determined using the well-known Lineweaver Burke plot (Shah, Dave, and Rao 2012; Agarry, Audu, and Solomon 2009; Waldrop 2009a; Lineweaver and Burk 1934) (or double reciprocal method) as per the Eq. 4.8 given as follows:

$$\frac{1}{\mu^{bg}} = \frac{K_d}{\mu_{max}^{bg}}\frac{1}{S} + \frac{1}{\mu_{max}^{bg}} \tag{4.8}$$

Where K_d is the half-saturation constant, and μ_{max}^{bg} is the maximum specific growth rate. The specific growth rate (μ^{bg}) are calculated at various initial dye concentrations using Eq. 4.4 (for the accelerating log phase where the presence of toxic metabolites is not considered) and Eq. 4.5 (for the entire log phase). The nature of inhibition in the decelerating log phase is determined by comparing the changes in the magnitudes of K_d and μ_{max}^{bg} for the entire log phase w.r.t the same obtained for the exponential accelerating phase.

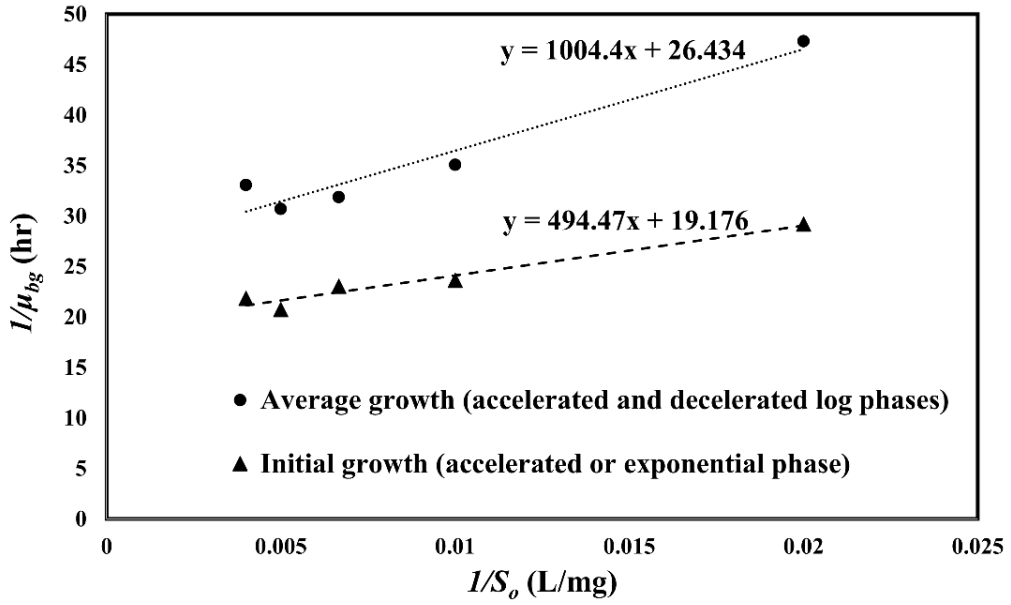

Figure 4.6 The inverse of growth rate ($1/\mu^{bg}$) vs the inverse of initial dye concentration ($1/S_o$) to determine the nature of enzyme inhibition in the decelerating log phase

Figure 4.6Figure 4.6 The inverse of growth rate ($1/\boldsymbol{\mu^{bg}}$) vs the inverse of initial dye concentration ($1/\boldsymbol{S_o}$) to determine the nature of enzyme inhibition in the decelerating log phase shows the inverse of initial-/and average-specific bacterial growth rates plotted against the inverse of initial dye concentrations. When the decelerated log phase was included, the magnitude of μ_{bg}^{max} fell from 0.052 to 0.037 mg/L, whereas the magnitude of K_d increased from 25.78 to 38 mg/L. The decrease in μ_{bg}^{max} and increase in K_d indicate the development of enzyme-substrate-inhibitor (ESI) complexes as a result of the substrate and inhibitor (metabolic toxicant in our investigation) binding to the enzyme simultaneously. The decelerating log phase shows a non-competitive kind of enzyme inhibition induced by hazardous metabolites. Due to the presence of azo-reductase and laccase enzymes, biphenyl and naphthalene (as shown in Figure 4.7) are generated during the biodegradation of Congo red dye (Hans et al. 2020). These are toxic and carcinogenic aromatic hydrocarbon compounds. Naphthalene causes cancer of the larynx and intestines in humans. The effect of these compounds particularly depends upon the exposure routes and their levels.

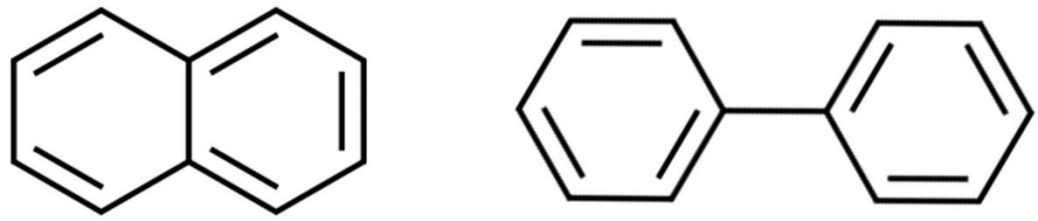

Figure 4.7 Molecular structure of key degradation products: (a) naphthalene; (b) biphenyl

4.5.4 Incorporation of time-averaged bacterial growth rate accounting metabolite inhibition in the bacterial growth models with substrate inhibition

The presence of high dye (i.e. substrate) concentration can inhibit the bacterial growth which was evident from the prolonged lag phase observed in Figure 4.4 and also discussed in

section 4.5.1. In this study, three well-known substrate inhibition models, Andrew-Haldane, Aiba and Edwards were used to model the inhibition at high substrate concentration. Conventionally, a constant specific growth rate, μ_a^{bg}, (obtained from Eq. 4.4) is used in these substrate inhibition model equations. However, in this study, a time-averaged specific growth rate for the entire log phase, μ_{avg}^{bg}, (obtained from Eq. 4.5) was used in all three substrate inhibition model equations (as presented in Table 4.3) to account for both, the metabolite inhibition of the decelerating log phase, and the substrate inhibition. The values of μ_{avg}^{bg} are determined using the data presented in Figure 4.4, and plotted against different initial dye concentrations in Figure 4.5. All three substrate inhibition models were fitted through non-linear regression with the measured μ_{avg}^{bg} *vs.* dye concentration data to determine model parameters. The substrate concentration that yields the maximum specific growth rate and beyond which the substrate inhibition becomes significant is known as critical substrate concentration, S_{crit}. The analytical expressions of S_{crit} for all three substrate inhibition models were determined in this study and summarized in Table 4.3.

It is apparent from Figure 4.7 that all three inhibitory kinetic models, in contrast to the non-inhibitory Monod's model, fit very well with the experimentally determined data of μ_{avg}^{bg} at different initial dye loadings. The parameters for all three inhibitory kinetic models along with the S_{crit} were determined and have been summarized in Table 4.3. The magnitude of inhibition parameters obtained from three inhibition models differed because of different origins and underlying assumptions adopted in these models. Since all the three models turned out to be fitting the experimental data very well as can be seen in the Figure 4.7, the values of S_{crit} were found to be similar for all three substrate inhibition models in the range of 169.5 to 172.8 mg/L. It implies that the substrate inhibition would dominate only if the dye concentration exceeds beyond this range. Finally, all three substrate inhibition models with their corresponding inhibition parameters listed in Table 4.3 can be used to predict the μ_{avg}^{bg}

(over the entire log phase) of *Bacillus Subtilis* MN372379 in the degradation of Congo Red dye.

Table 4.3 Kinetic parameters obtained by fitting the experimental data (μ_{avg}^{bg} vs S_o) with various substrate inhibition models

Model	Equation (Incorporating time-averaged bacterial growth rate)	Inhibition parameters	Critical substrate concentration
Andrew Haldane Model	$\mu_{avg}^{bg} = \frac{\mu_o^{bg,AH} S}{K_{d,AH} + S + \frac{S^2}{K_{I,AH}}}$	$\mu_o^{bg,AH} = 0.092\ hr^{-1}$, $K_{d,AH} = 145.97\ mg/L$, $K_{I,AH} = 196.74\ mg/L$	$S_{crit} = \sqrt{K_{d,AH}.K_{I,AH}}$ $= 169.46 mg/L$
Aiba Model	$\mu_{avg}^{bg} = \mu_o^{bg,A} \frac{S}{S + K_{d,A}} exp\left(-\frac{S}{K_{I,A}}\right)$	$\mu_o^{bg,A} = 0.097 hr^{-1}$, $K_{d,A} = 142.28\ mg/L$, $K_{I,A} = 382.66\ mg/L$	S_{crit} $= \frac{1}{2}\left(-K_{d,A} + \sqrt{{K_{d,A}}^2 + 4K_{d,A}.K_{I,A}}\right)$ $= 172.8\ mg/L$
Edwards Model	$\mu_{avg}^{bg} = \mu_o^{bg,E}\left[exp\left(-\frac{S}{K_{I,E}}\right) - exp\left(-\frac{S}{K_{d,E}}\right)\right]$	$\mu_o^{bg,E} = 0.047\ hr^{-1}$, $K_{d,E} = 65.93 \frac{mg}{L}$ $K_{I,E} = 688.78\ mg/L$	S_{crit} $= \left(\frac{1}{K_{d,E}} - \frac{1}{K_{I,E}}\right) \Big/ \ln\frac{K_{I,E}}{K_{d,E}}$ $= 171.08\ mg/L$

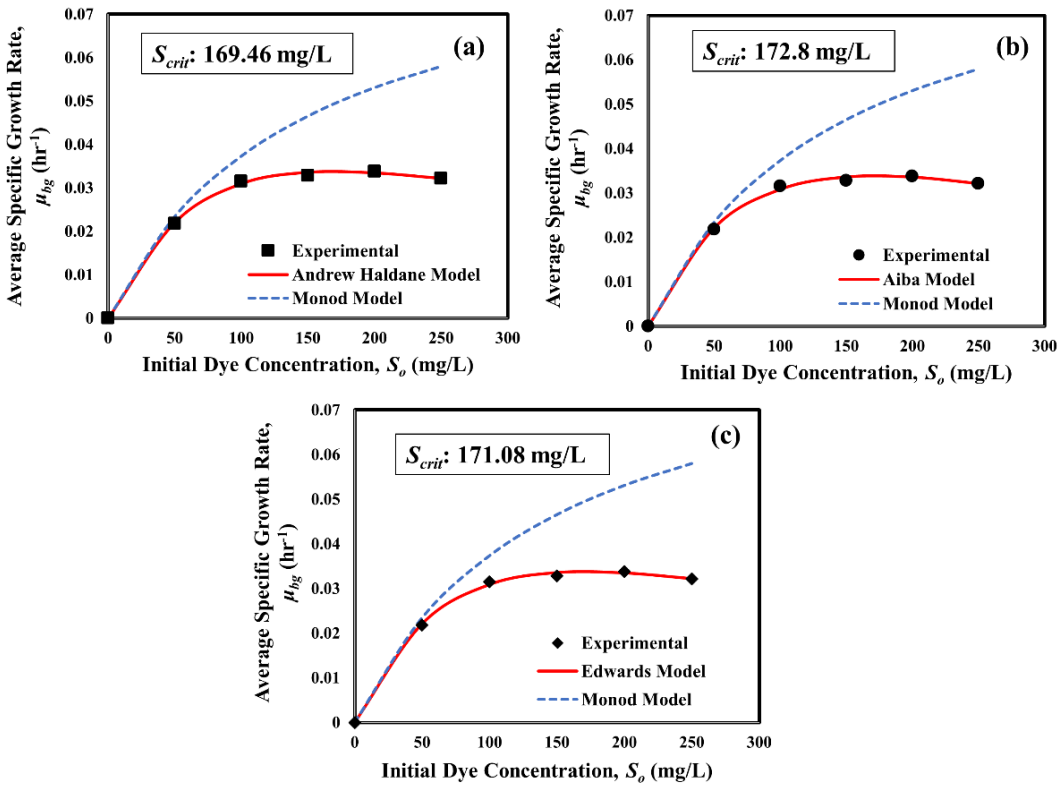

Figure 4.8 Comparison of average specific growth rates (μ_{avg}^{bg}) obtained from experiments at various initial dye concentrations with the substrate inhibitory models: (a) Andrew-Haldane model; (b) Aiba model, and (c) Edwards model. The dotted line presents the non-inhibitory Monod's model

4.6 Process optimization for the maximum dye utilization

4.6.1 Optimization of the initial dye concentration

Optimizing a biodegradation reaction aims to find the process parameters that allow for the most efficient substrates/targeted pollutants. The substrates (in this case, Congo Red dye) should ideally be used as feed by the bacterial mass throughout their metabolic activities. As a result, the best dye concentration for maximal degradation should be chosen.

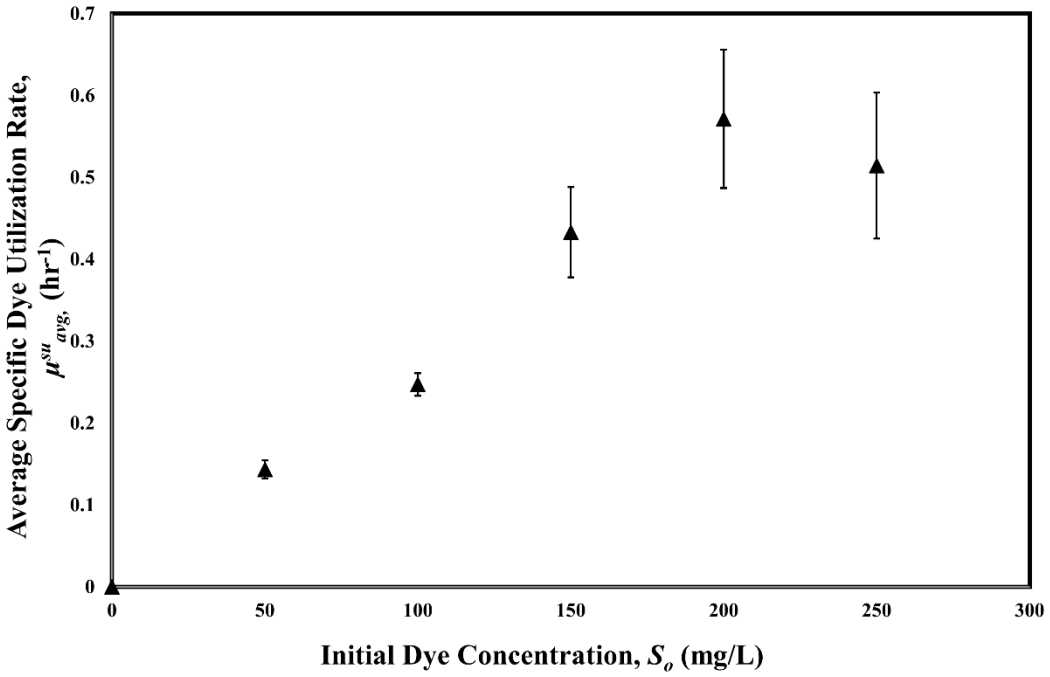

Figure 4.9 Average specific dye (substrate) utilization rate, μ^{su}_{avg}, obtained from Eq 4.7 against different initial dye concentrations

Figure 4.9 illustrates the average specific substrate utilization rate, μ^{su}_{avg} (defined as the time-averaged mass of dye removed per unit time per unit bacterial mass) for an initial inoculum size of 7.68×10^8 CFU/mL with different beginning dye concentrations (S_o). Eq 4.7 was used to compute the μ^{su}_{avg} for the full log phase at varying S_o. At a dye concentration of 200 mg/L, the greatest specific dye utilization rate of 0.57 hr^{-1} was found. The decrease in μ^{su}_{avg} beyond 200 mg/L of S_o is due to bacterial growth inhibition caused by high substrate loading, as stated in Sec. 4.5.4. Figure 4.5 and Figure 4.9 show that the average bacterial growth rate and dye usage rate follow a similar pattern, reaching their peaks near the same initial dye concentration of 200 mg/L. The isolated bacterial strain Bacillus Subtilis MN372379 may use Congo Red dye as a primary energy source in its metabolic activities.

4.6.2 Optimization of the initial inoculum size

Different inoculum sizes of 1.92×10^8, 3.84×10^8, 7.68×10^8 and 11.52×10^8 CFU/mL were used in this investigation to optimize the starting count of bacterial cells for maximal

dye utilization. The influence of inoculum size on bacterial growth and dye usage rate is shown in Figure 4.10. At an initial dye concentration of 50 mg/L, Figure 4.10(a) depicts the bacterial concentration over time as the initial inoculum size was increased from 1.92×10^8 CFU per mL to 11.52×10^8 CFU/mL. It's evident and expected that a large initial inoculum size would result in a high biomass concentration. Additionally, the lag phase was reduced when the initial inoculum size was increased. Increasing the inoculum size reduces the relative substrate toxicity for the bacterial population, allowing cells to adjust to the dye environment and begin their multiplication quickly.

Furthermore, the size of the initial inoculum has an impact on the rate of substrate utilization. Figure 4.10 (b) and Figure 4.10 (c) show the average dye utilization and average specific dye utilization rates with varying inoculum sizes and beginning dye concentrations. The increase in the average dye utilization rate (-dS/dt) with increasing initial inoculum sizes is apparent and predicted, as illustrated in Figure 4.10. This is due to increased bacterial population at large inoculum sizes (as seen in Figure 4.10 (a)).

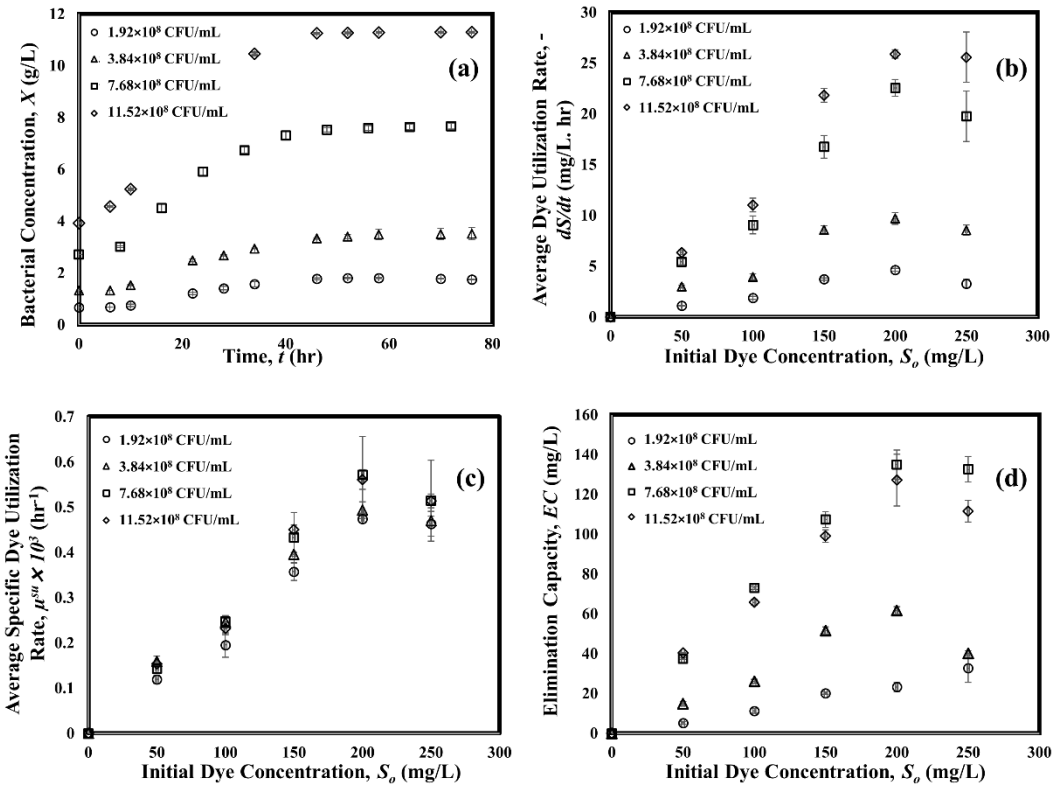

Figure 4.10 Effect of the initial inoculum size: (a) Bacterial concentration vs. time; (b) Average dye utilization rate, (c) Average specific dye utilization rate, and (d) Elimination capacity are plotted at different initial dye concentrations

Furthermore, beyond a critical inoculum size (7.68×10^8 CFU/mL in this work), the average specific dye utilization rate (*-dS/X.dt*, calculated using Eq. 4.7 and displayed in Figure 4.10 (c)), was found to be nearly equal. It shows that the dye utilisation rate *(-dS/dt)* grows linearly above a critical inoculum size with the bacterial concentration *(X)*. Finally, the dye elimination capacity (EC) is shown in Figure 4.10 (d), which is defined as the mass of net dye eliminated per unit volume of the reaction mixture as follows:

$$EC = S_{initial} - S_{final} \qquad (4.9)$$

When the initial inoculum size was increased from 1.92×10^8 CFU/mL to 11.52×10^8 CFU/mL, the elimination capacity also increased. However, at large inoculum sizes (more than 7.68×10^8 CFU/mL in this investigation), the relative gain in elimination capacity was shown to diminish. This is because competition for substrate (in this example, dye) becomes more

intense at large inoculum sizes. It reduces the relative gain in the elimination capacity beyond a critical inoculum size. As a result, while optimizing the biodegradation process, the parameters (such as initial dye loading and bacterial mass concentration, for example) should be selected so that the *average specific dye-utilization rate* and *dye-elimination capacity* are maximized, allowing for maximal dye utilization.